

# NEUTRINO OSCILLATIONS RESULTS FROM MINOS

K. LANG <sup>a</sup>

*Department of Physics, 1 University Station C1600,  
The University of Texas, Austin, Texas 78712-0264, USA*

The MINOS experiment at Fermilab has completed its first year of operations with an intense neutrino beam from Main Injector. Neutrino interactions registered by MINOS were produced by  $1.27 \times 10^{20}$  protons with momentum 120 GeV/c striking a graphite target. Analysis of charged current interactions in the two detectors reveals the disappearance of muon-type neutrinos on their way from Fermilab to the Soudan mine 734 km away with  $6.2\sigma$  significance. The effect is well described by two-neutrino oscillations with best-fit mixing parameters  $|\Delta m_{32}^2| = (2.74 \pm_{0.26}^{0.44}) \times 10^{-3} eV^2/c^4$  and  $\sin^2 2\theta_{23} = 1.00_{-0.13}$ , where errors reflect the statistical and systematic uncertainties of the measurement.

## 1 Introduction

The MINOS experiment <sup>2</sup> was conceived about a dozen years ago in the midst of emerging hints of neutrino oscillations. Although the phenomenon was discovered and confirmed by other experiments, <sup>3,4,5,6</sup> the motivation for MINOS is still compelling since the strategy of the experiment offers the possibility of achieving small systematic uncertainties of neutrino oscillations measurements.

MINOS is a long baseline, two-detector experiment which uses a high intensity, well-controlled neutrino beam. The beam energy is optimized for muon-neutrino disappearance and electron-neutrino appearance to be measured by two detectors separated by a distance of 734 km. Given this distance and the value of  $\Delta m_{32}^2$  of about  $(1.5 - 3.5) \times 10^{-3} eV^2/c^4$ , indicated previously, the effect of neutrino oscillations occurs mostly for neutrinos with energies in the (0.5 – 5) GeV range. Neutrino interactions at these energies are experimentally more challenging for the MINOS detectors than interactions at higher energies and effectively rule out the observation of the appearance of tau-neutrinos in MINOS.

Results presented here are based on the first year of MINOS beam exposure from May 2005 to March 2006. Since the first beam results have been recently published <sup>7</sup>, here we only briefly outline the key analysis steps and provide supplemental information on the MINOS measurement.

## 2 The NuMI beam line

MINOS was designed together with a new neutrino beam line, NuMI, <sup>8</sup> which uses protons with momentum 120 GeV/c from Fermilab's Main Injector (MI). A schematic layout of the beam is shown in Figure 1. The key elements of the beam line is a segmented 95.4 cm long graphite

---

<sup>a</sup>On behalf of the MINOS Collaboration <sup>1</sup>

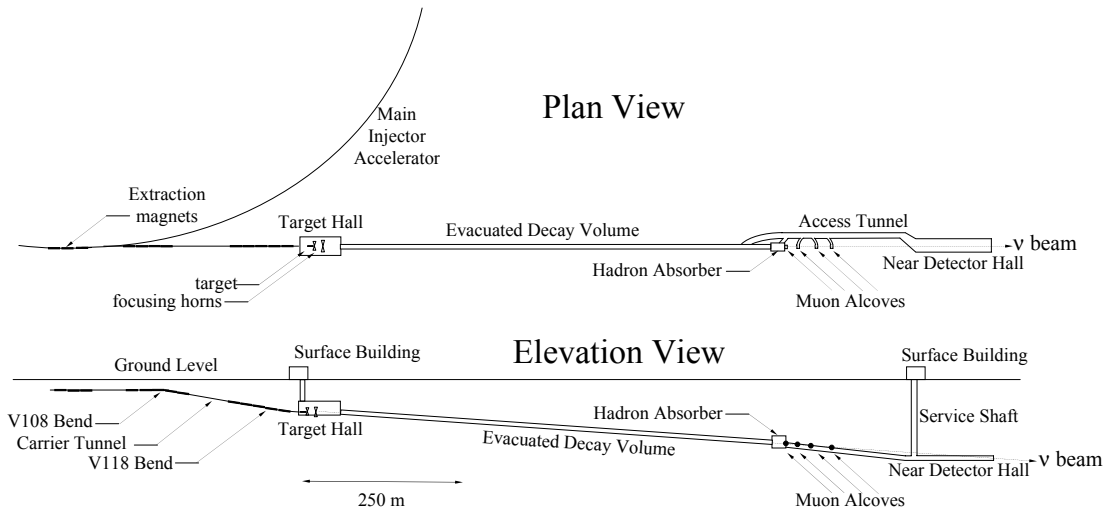


Figure 1: A schematic view of the NuMI neutrino beam line with the main focusing, beam monitoring elements, and the Near detector.

target and a pair of pulsed parabolic magnetic horns, which are used to produce and focus secondaries, as it is illustrated in Figure 2. Every (2.0 – 2.6) s, MI delivers a beam of about  $(2.2 - 2.5) \times 10^{13}$  protons per pulse in 5 or 6 batches, each about  $1.56 \mu\text{s}$  long. The beam line elements, together with a 675 m long evacuated decay pipe, point  $3.3^\circ$  downward toward the Far detector located in the Soudan mine in Minnesota. The Near detector is located about 300 m downstream of the beam stop and secondary beam monitors.<sup>9</sup>

The NuMI target can be moved remotely along the axis of the beam within a range of 250 cm. To focus the lowest energy secondaries, the target can be inserted into the first horn almost to its “neck”; the highest energy secondaries are focused for the most upstream position of the target. Different target-horn configurations yield neutrino beams peaking at different energies. Monte Carlo simulations of the neutrino fluxes and resulting energy spectra of charged current interactions for three main beam configurations are shown in Figures 3 and 4. Table 1 lists all horn currents and target positions with which MINOS took data, together with an expected number of events in the Far detector per  $1 \times 10^{20}$  protons on target (POT) assuming no oscillations.

The flexibility of the target-horn arrangement and different horn current settings provided crucial information in adjusting the hadron production modeling employed in MINOS Monte Carlo simulations. As Table 1 shows, most of exposure MINOS took at the lowest energy setting to maximize the number of oscillating neutrinos.

Table 1: Summary of NuMI beam configurations and their main features. The number of expected muon-neutrino charged current events is calculated for an ideal 5.4 kton detector per  $1 \times 10^{20}$  POT.

Beam setting name	Target from the “neck” (cm)	Horn current (kA)	Exposure May’05-Mar’06 ( $10^{18}$ POT)	Peak $E_\nu$ (GeV)	No. of events in an ideal Far det. (no oscillations) per $1 \times 10^{20}$ POT
LE-10/0	10	0	2.69	9.0	156
LE-10/170	10	170	1.34	3.0	385
LE-10/185	10	185	127.0	3.0	428
LE-10/200	10	200	1.26	3.2	474
LE-100/200	100	200	1.11	5.2	861
LE-250/200	250	200	1.55	10.2	1,275

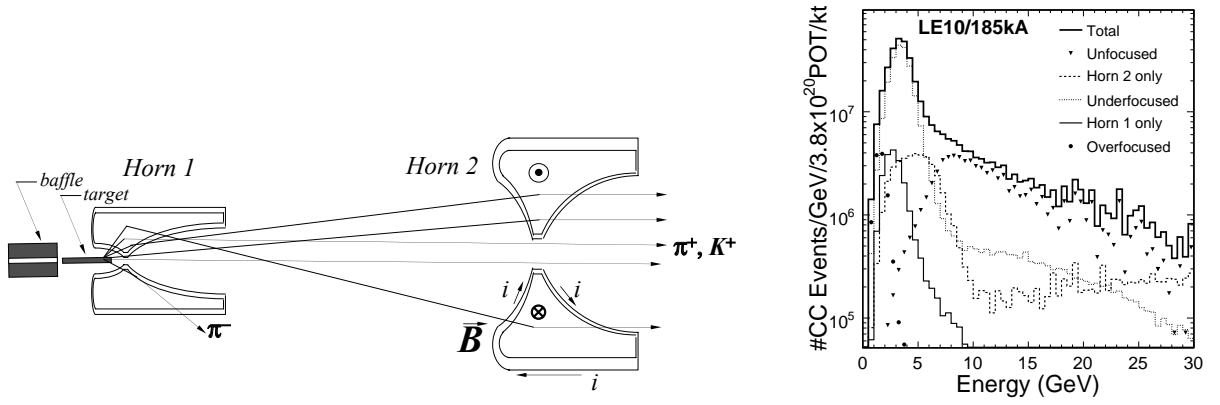


Figure 2: The left figure illustrates the focusing of the secondary beam by the two-horn NuMI system. Monte Carlo predictions of the resulting Near detector charged current energy spectra for the LE-10/185 beam setting and its focusing components are shown in the right panel.

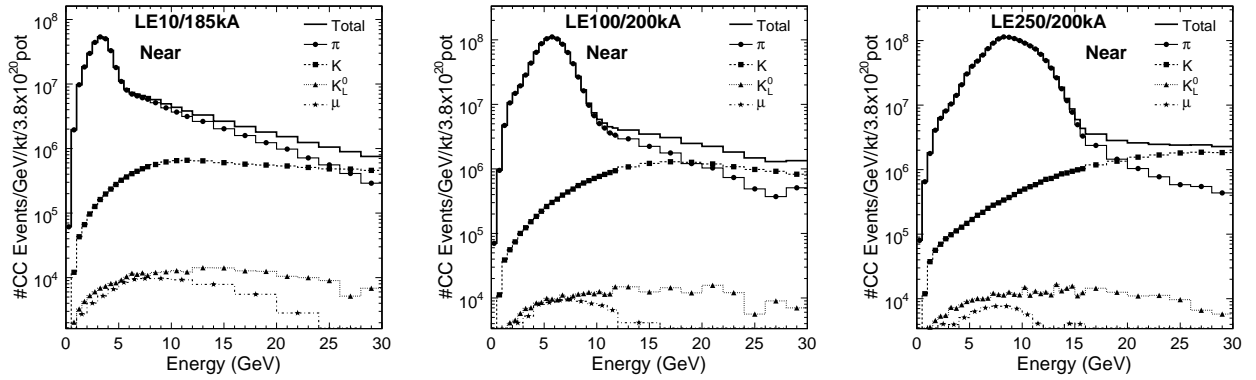


Figure 3: Monte Carlo calculations of the Near detector muon-neutrino charged current energy spectra and its composition for the three main beam settings LE-10/185, LE-100/200, and LE-250/200.

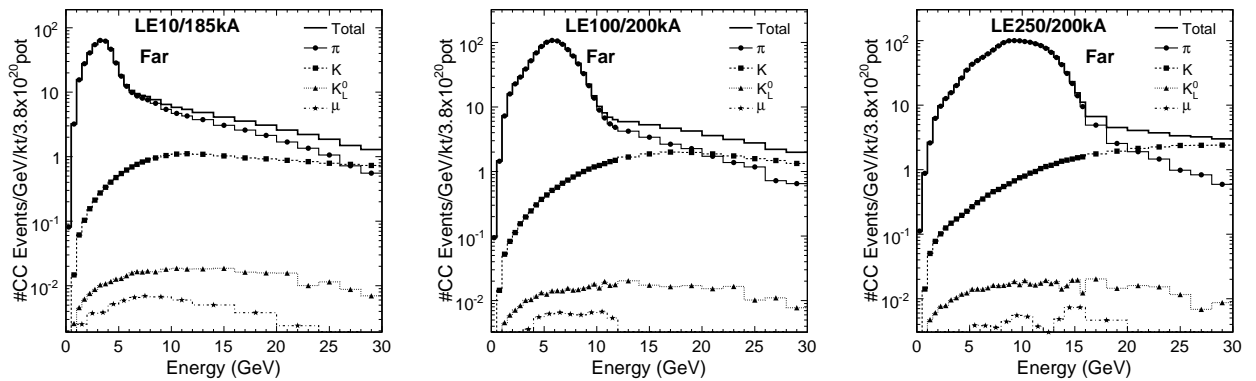


Figure 4: Monte Carlo calculations of the Far detector muon-neutrino charged current energy spectra and its composition for the three main beam settings, LE-10/185, LE-100/200, and LE-250/200, and under an assumption of no neutrino oscillations.

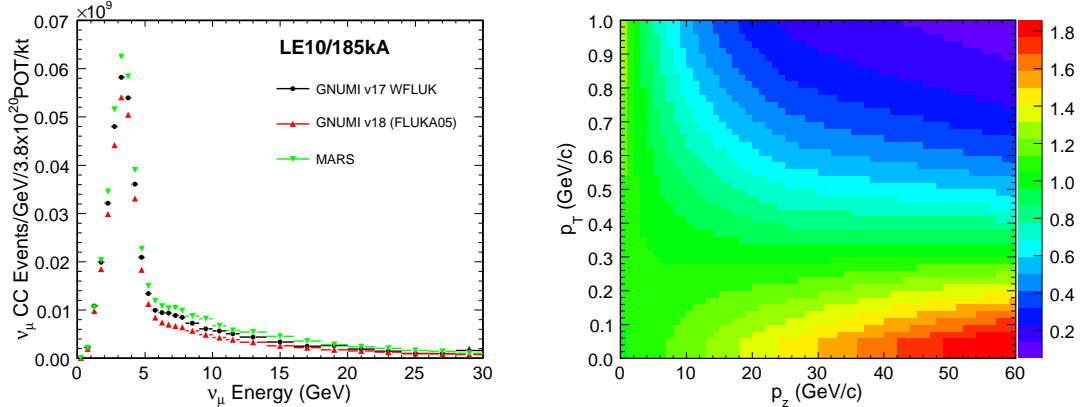


Figure 5: Left: Comparison of hadron production using three different models. Right: Monte Carlo tuning corrections (“weights”) of FLUKA05 in the  $p_z - p_T$  plane. In the region of most interest ( $p_z < 10$  GeV and  $p_T < 0.5$  GeV) the weights are close to 1 but significantly improve the agreement of simulations with data.

### 3 Two detectors

The two functionally-identical MINOS detectors are tracking calorimeters employing 2.54 cm thick steel plates and 4.1 cm wide extruded plastic scintillator strips which form octagonal toroids, magnetized for muon charge selection.<sup>10</sup> The 5.4 kton Far detector is located 705 m underground in the Soudan mine, while the 1 kton Near detector is placed on Fermilab’s site about 1 km from the target and 103 m underground. Scintillation light is collected with wavelength-shifting fibers and multi-anode photo-multiplier tubes (PMT)<sup>12</sup>. PMT signals are digitized and read out effectively continuously with no loss of hits during an accelerator spill. Muons crossing the detectors yield about 8-12 photoelectrons per plane and the detectors achieve the hadronic energy resolution of  $56\%/\sqrt{E(\text{GeV})} \oplus 2\%$  and the electromagnetic energy resolution of  $21.4\%/\sqrt{E(\text{GeV})} \oplus 4.1\%$ <sup>11</sup>. Muons which stop in the detectors have their energy determined from the range with a 6% resolution, while the energy of exiting tracks is determined with about 13% resolution from the curvature in the toroidal magnetic field.

Both detectors operate extremely reliably and routinely with a duty factor  $> 98\%$ . Only at very low light levels the detectors suffer from noise from natural radioactivity, spontaneous fiber light emission, and the PMT dark current<sup>13</sup>. Due to granularity, the efficiency for registering a muon-neutrino charged current interaction below 1 GeV is about 30%.

### 4 The data

MINOS took data with 6 beam configurations listed in Table 1. It is well known that Monte Carlo simulations of neutrino fluxes strongly depend on the underlying models of hadron production, as illustrated in Figure 5, which are presently poorly constrained at MINOS energies. We used FLUKA05 model in our calculations. The nominal simulations yielded energy spectra which did not match the high-statistics data in the Near detector. A better agreement was achieved by smoothly adjusting the  $p_z$  and  $p_T$  of hadrons (mostly pions) produced off the graphite target. The tuning corrections (“weights”) are shown in Figure 5, and the resulting spectra, which describe the data much more closely than the nominal simulations, are shown in Figure 6.

Several requirements of the integrity and good quality of NuMI beam spills and both detector events were applied as a pre-selection procedure. Only a small fraction of recorded data were rejected. For this first analysis of neutrino oscillations, only events produced by  $1.27 \times 10^{20}$  POT in the LE-10/185 target-horn configuration were used.

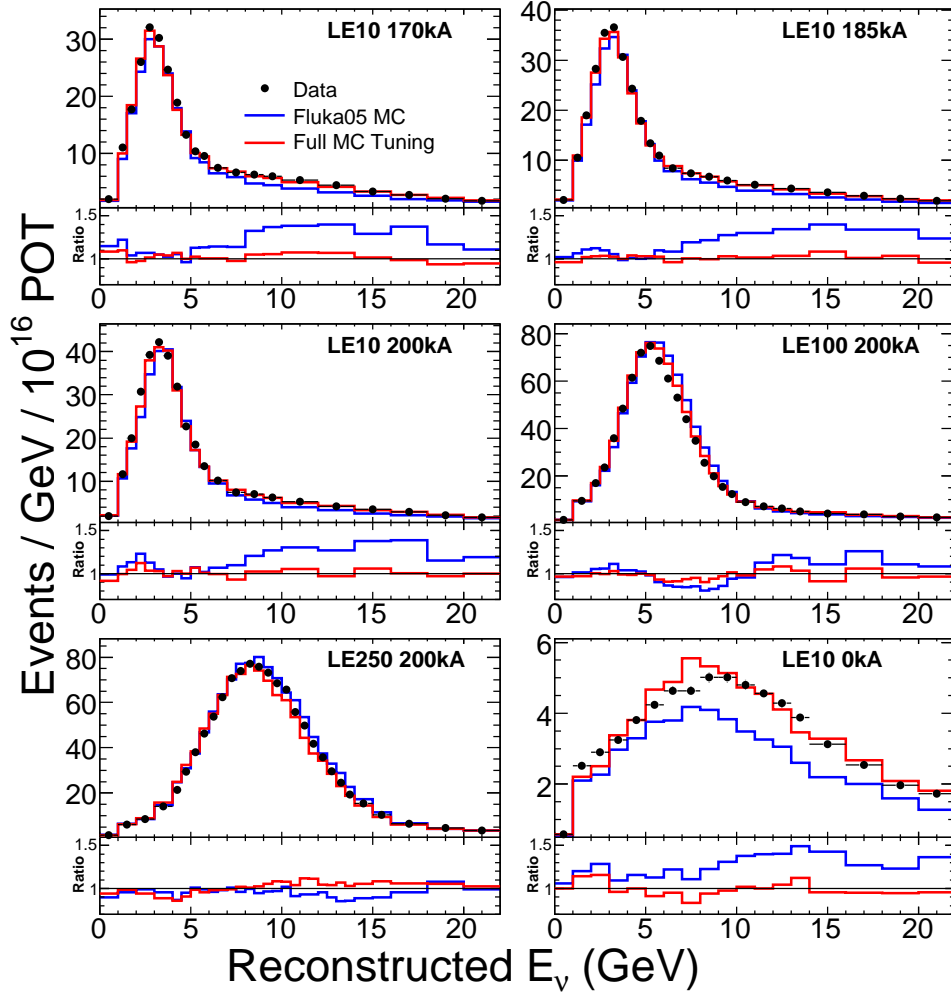


Figure 6: Energy spectra in the MINOS Near detector for the six beam configurations listed in Table 1. The lower insets show the ratios of data to Monte Carlo before and after tuning of the hadron production.

## 5 Analysis and results

All well reconstructed events were classified either as neutral current or charged current neutrino interactions using a probability distribution function (PDF) obtained from three quantities derived for each event. These quantities and the resulting PDF for the Near detector are shown in Figure 7. Corresponding Monte Carlo quantities, also shown in this figure, are based on the tuned hadron production model. In addition, the sign of the muon charge, determined from the trajectory in the toroidal magnetic field, was required to be negative, thus selecting muon-neutrino charged current interactions.

The large data set in the Near detector was used to verify that the detector and the beam operated as expected and that the most important detector and beam features were well modeled by Monte Carlo. Data in the Far detector were not available in its entirety due to a blind analysis approach. However, an open data set, an unknown fraction of the full data set selected by a blinding algorithm, was sufficient to conduct a number of significant checks of the integrity of data registered by the Far detector. Only after all analysis steps and final event selections were determined on the basis of the Near detector data and the Far and Near detector Monte Carlo events, the complete data set in the Far detector was processed through the full analysis chain.

There were three main steps of the analysis. First, the energy spectrum of charged current muon-neutrinos in the Near detector was determined. Second, the Near detector energy spec-

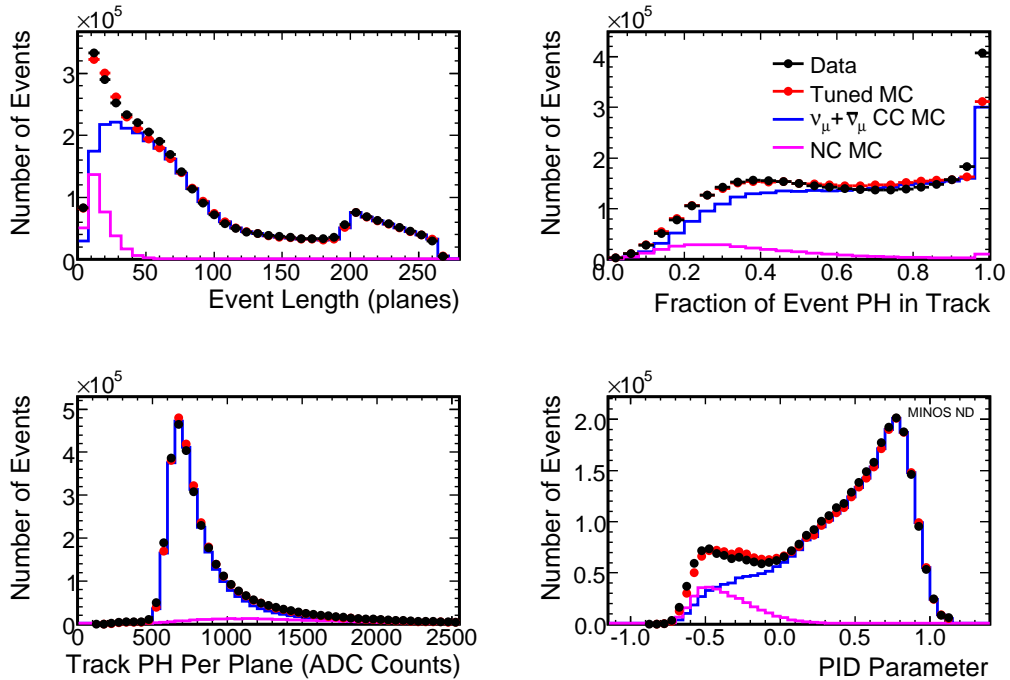


Figure 7: Near detector data and Monte Carlo predictions for the event length, the track per event pulse-height fraction, and the average pulse-height per track plane. The probability distribution function derived from these quantities is shown in the lower right panel. Charged current-like events cluster around  $\text{PID}=1$ , while neutral current-like events are close to  $\text{PID}=0$ . Similar event classification is achieved for the Far detector.

trum was then used to predict the energy spectrum to be observed at the Far detector without neutrino oscillations. In the last step, the *predicted* spectrum was compared to the actually *measured* spectrum.

We used two different approaches for predicting the Far detector spectrum. In the “beam matrix” method, after Monte Carlo corrections of inefficiencies, the spectrum of *true* neutrino energy was projected, using kinematics and the beam line geometry, to the Far detector, where it was then unfolded to a *measured* energy spectrum. In the “NDFit” method, Monte Carlo was additionally tuned to better agree with the Near detector data. Such adjusted model was then used to generate the Far detector spectrum. The two techniques have different sensitivities to systematic uncertainties in modeling the experimental setup and neutrino interactions but produce very similar results shown in Figure 8. We chose the beam matrix as the “official method”. Table 2 shows the number of observed and expected events in three energy ranges. The disappearance of muon-neutrinos is measured with a  $6.2\sigma$  significance.

Table 2: The number (and its uncertainty) of expected muon-neutrino charged current (CC) events in the Far detector for the LE-10/185 beam configuration using the beam matrix prediction with no neutrino oscillations, and the number of observed events for three energy ranges.

Energy range of CC events	No. of expected CC events in Far (no oscillations)	No. of observed CC events in Far
$< 30$ GeV	$336.0 \pm 14.4$	215
$< 10$ GeV	$238.7 \pm 10.7$	122
$< 5$ GeV	$168.4 \pm 8.8$	76

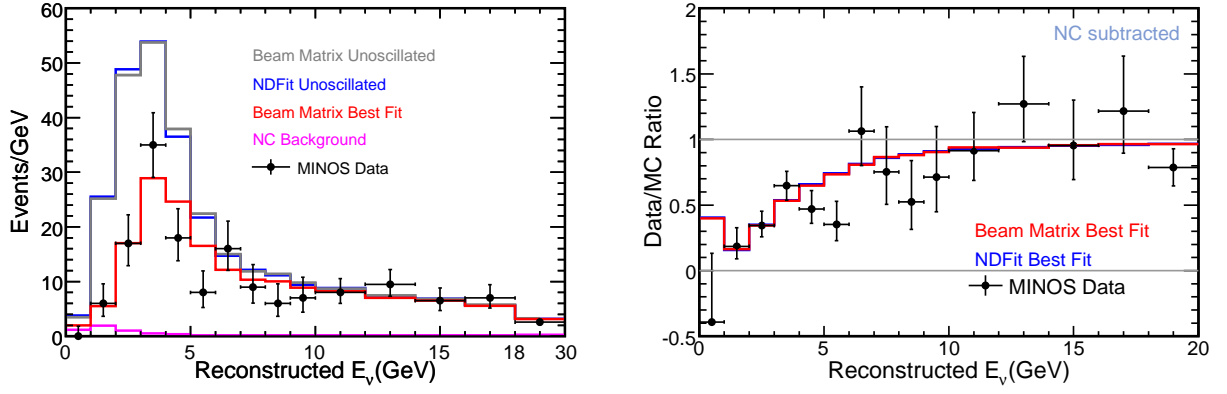


Figure 8: Left: Final comparison of the Far detector energy spectrum with predictions for no oscillations for both analysis methods. Also shown is the spectrum with oscillations with the best-fit parameters from the beam matrix method. The estimated neutral current (NC) background is also shown. The last energy bin contains events between 18-30 GeV. Right: Ratio of MINOS data over Monte Carlo prediction for no oscillations.

Table 3: A summary of systematic uncertainties of the oscillation parameters.

Uncertainty	Level of uncertainty	$\Delta m_{32}^2$ ( $10^{-3} \text{ eV}^2/c^4$ )	$\sin^2 2\theta_{23}$
Near/Far normalization	$\pm 4\%$	0.050	0.005
Absolute hadronic energy scale	$\pm 11\%$	0.060	0.048
NC contamination	$\pm 50\%$	0.090	0.050
All other systematic uncertainties		0.044	0.011
Total systematic uncertainty (summed in quadrature)		0.12	0.07
Statistical error (data)		0.36	0.12

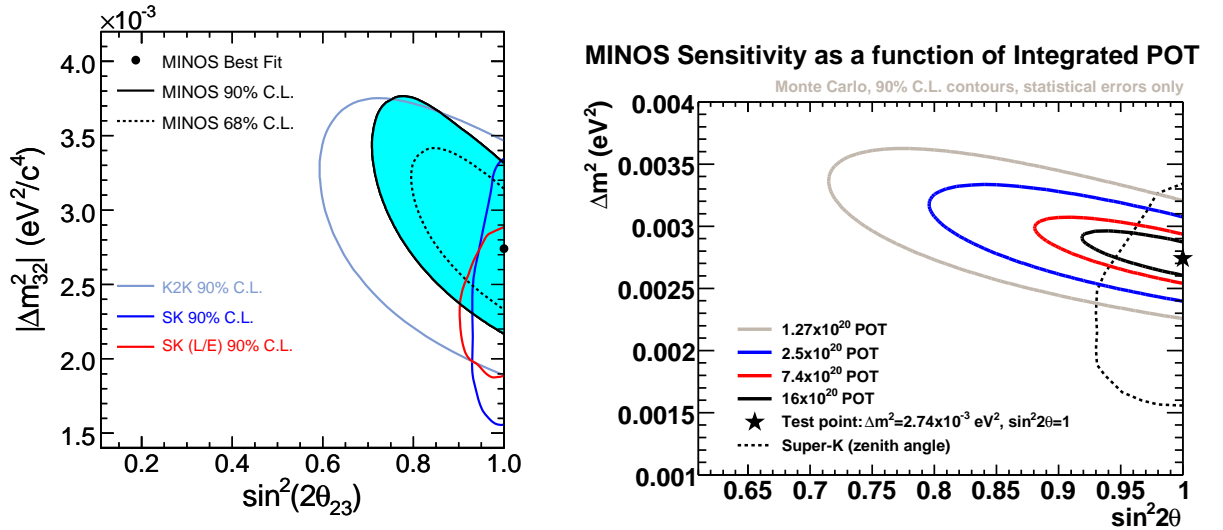


Figure 9: Left: Confidence intervals for the fit to the MINOS data using the beam matrix method including systematic errors. Also shown are the contours from the previous highest precision experiments Super-K and K2K. Right: MINOS sensitivity as a function of the number of protons on the NuMI target.

The difference between the predicted and observed energy spectra was used to measure the neutrino mixing parameters. This was achieved by generating predicted spectra with different neutrino oscillation parameters. The spectrum matching best was obtained for  $|\Delta m_{32}^2| = (2.74 \pm_{-0.26}^{+0.44}) \times 10^{-3} \text{ eV}^2/c^4$  and  $\sin^2 2\theta_{23} = 1.00 \pm_{-0.13}$ , where errors reflect the statistical and systematic uncertainties of the measurement summarized in Table 3. The resulting parameter contours are shown in the left panel of Figure 9.

## 6 Summary and outlook

Within the first year of running, MINOS collected neutrino data produced by  $1.27 \times 10^{20}$  protons on target. Analysis of the muon-neutrino charged current interactions proves the disappearance of muon-neutrinos on their 734 km long way from Fermilab to the Soudan mine. For neutrinos with energy less than 10 GeV,  $238.7 \pm 10.7$  events were expected in the Far detector if no oscillations are assumed, while 122 were observed. The disappearance of events and their energy spectrum yield the best-to-date measurement of the mixing parameter  $|\Delta m_{32}^2| = (2.74 \pm_{-0.26}^{+0.44}) \times 10^{-3} \text{ eV}^2/c^4$ , where the errors reflect the statistical and systematic uncertainties of the measurement.

MINOS has resumed data taking after the Summer 2005 accelerator shutdown. The collaboration continues advancing several other analyses, e.g., of electron-neutrino appearance, neutral current Far to Near detector energy spectrum comparison, neutrino time-of-flight, neutrino cross-sections, and more, so within the next several months new results will become available. In the future, the sensitivity of MINOS to neutrino oscillations will strongly depend on the number of protons delivered on the NuMI target, as it is illustrated in the right panel of Figure 9.

## Acknowledgments

I would like to thank the organizers of this conference for providing an excellent selection of topics and speakers and a stimulating scientific atmosphere in an unforgettable setting of Hanoi and its people. This work was supported in part by grant DE-FG03-93ER40757 of the US Department Energy.

## References

1. The MINOS Collaboration includes research groups from 32 institutions. Details are available at <http://www.numi.fnal.gov>.
2. Fermilab Proposal P875, February, 1995;  
*The MINOS Detectors*, Technical Design Report, Fermilab, NuMI-L-337, October, 1998.
3. Y. Fukuda *et al.* [Super-Kamiokande Collaboration], *Phys. Rev. Lett.* **81**, 1562 (1998).
4. M. H. Ahn *et al.* [K2K Collaboration], *Phys. Rev. Lett.* **90**, 041801 (2003).
5. Q. R. Ahmad *et al.* [SNO Collaboration], *Phys. Rev. Lett.* **89**, 011301 (2002).
6. K. Eguchi *et al.* [KamLAND Collaboration], *Phys. Rev. Lett.* **90**, 021802 (2003).
7. D. G. Michael *et al.* [MINOS Collaboration], *Phys. Rev. Lett.* **97**, 191801 (2006).
8. S. Kopp, *The NuMI neutrino beam at Fermilab*, arXiv:physics/0508001 (2005).
9. S. Kopp *et al.*, *Nucl. Instrum. Methods* **A568**, 503 (2006);  
R. Zwaska *et al.*, *Nucl. Instrum. Methods* **A568**, 548 (2006).
10. K. Lang [for MINOS Collaboration], *Nucl. Instrum. Methods* **A461**, 290 (2001).
11. P. Adamson *et al.*, *Nucl. Instrum. Methods* **A556**, 119 (2006).
12. K. Lang *et al.*, *Nucl. Instrum. Methods* **A545**, 852 (2005);  
N. Tagg *et al.*, *Nucl. Instrum. Methods* **A539**, 668 (2005).
13. S. Avvakumov *et al.*, *Nucl. Instrum. Methods* **A545**, 145 (2005).